

Cell Reports, Volume 43

Supplemental information

Synaptic plasticity via receptor tyrosine

kinase/G-protein-coupled receptor crosstalk

Cristina Lao-Peregrin, Guoqing Xiang, Jihye Kim, Ipsit Srivastava, Alexandra B. Fall, Danielle M. Gerhard, Piia Kohtala, Daegeon Kim, Minseok Song, Mikel Garcia-Marcos, Joshua Levitz, and Francis S. Lee

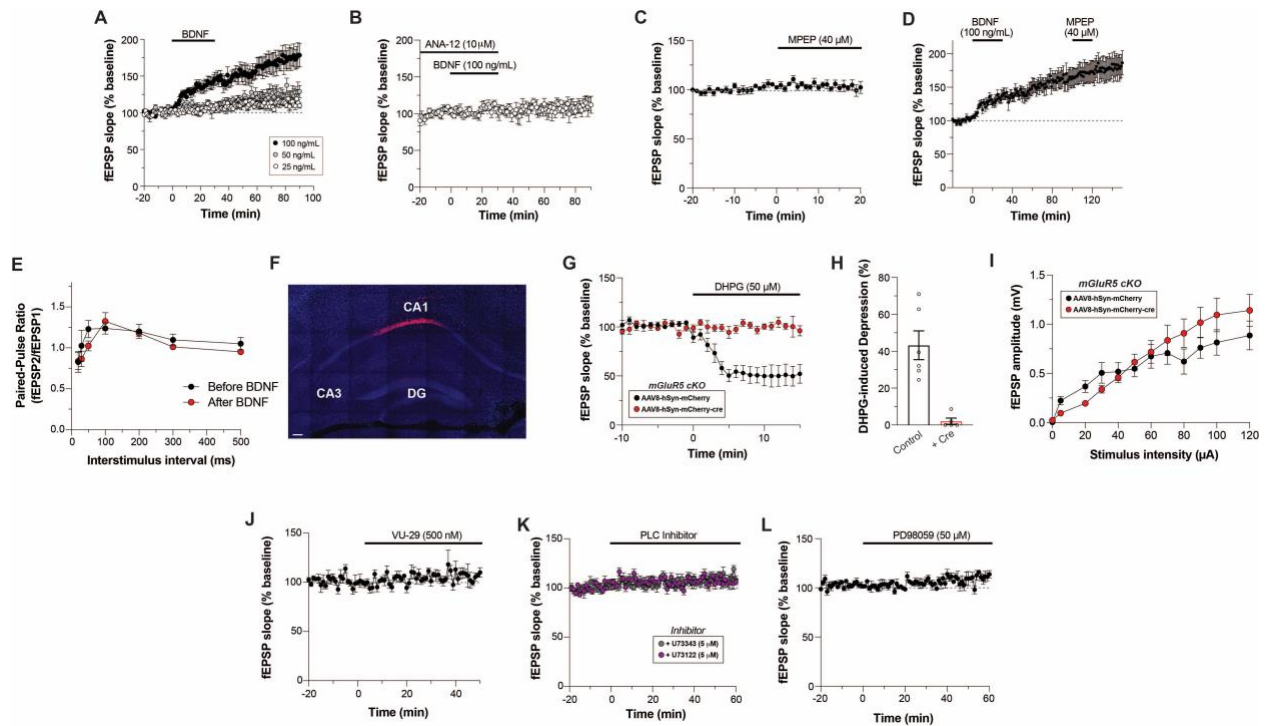


Figure S1. Further electrophysiological analysis of BDNF-LTP in hippocampal slices, related to Figure 1. (A) fEPSP slope time course in response to various doses of BDNF for 30 min (from Time = 0 to 30 min). 100 ng/mL (n = 8 slices), 50 ng/mL (n = 6 slices), 25 ng/mL (n = 5 slices). (B) fEPSP slope time course with ANA-12 alone showing no effects on baseline plasticity (n = 4 slices). (C) fEPSP slope time course with MPEP alone showing no effects (n = 5 slices). (D) fEPSP slope time course showing no effect of MPEP after BDNF-LTP induction and maintenance for 60 min (n = 6 slices). (E) Paired-pulse ratio of fEPSPs across a range of interpulse intervals before and after BDNF 100 ng/mL perfusion for 30 min (n = 6 slices). (F) Representative image of dorsal CA1 hippocampal expression of AAV8-hSyn-mCherry-Cre in mGluR5^{FL/FL} mice (CA1, CA3 = cornu ammonis 1, 3; DG = dentate gyrus, scale bar 100 μm). (G-H) DHPG application decreases fEPSP slope in control mGluR5^{FL/FL} slices with AAV8-hSyn-mCherry, but not when mGluR5 is knocked out with AAV8-hSyn-mCherry-Cre. Individual points in (H) denote independent slices taken from distinct mice, and unpaired student t-test is used. (I) Input/output curve of fEPSP amplitude under basal conditions in mGluR5^{FL/FL} mice with AAV8-hSyn-mCherry (n = 4 slices) or AAV8-hSyn-mCherry-Cre (n = 5 slices). (J-L) fEPSP slope time courses showing no effects of VU-29 (J, n = 6 slices), PLC inhibitor U-73122 or inactive analog U-73343 alone (K, n = 6 slices for each drug), or MEK inhibitor PD-98059 alone (L, n = 6 slices). For (A-L), each slice is taken from distinct mice. All data are shown as mean ± SEM.

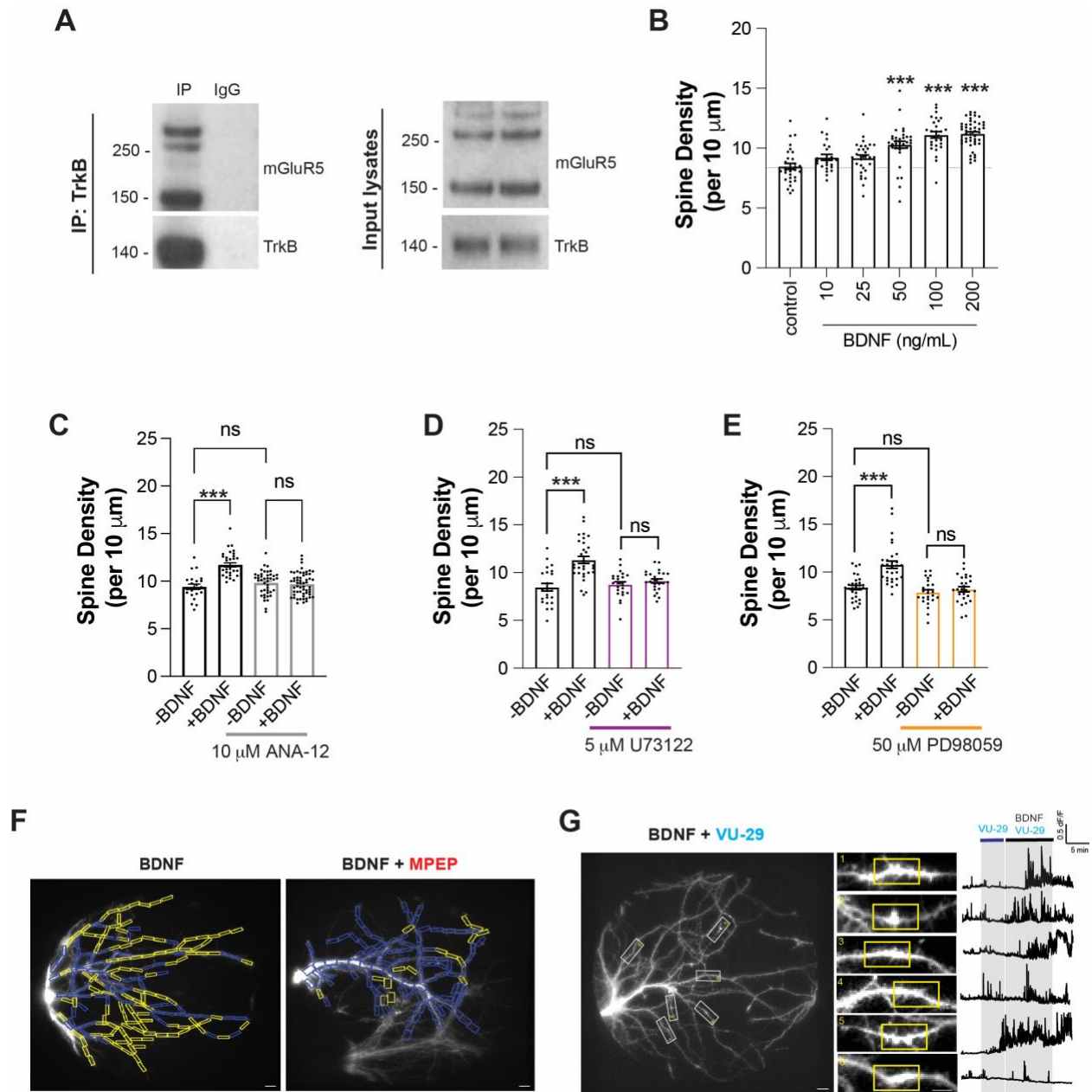


Figure S2. Further spine imaging and dendritic calcium imaging analysis, related to Figure 2. (A) Co-immunoprecipitation of endogenous TrkB and mGluR5 in DIV 19 primary hippocampal neuronal lysates. (B) Bar graphs showing dendritic spine density with increasing concentrations of BDNF for 30 min. (C-E) Bar graphs showing dendritic spine density without or with 100 ng/mL BDNF for 30 min with various pharmacological modulations. Pre-treatment with TrkB antagonist ANA-12 (C), PLC inhibitor U-73122 (D), or MEK inhibitor PD-98059 (E) for 60 min before 100 ng/mL BDNF addition prevents the BDNF-induced increase in spine density without altering basal spine density. For (B-E), individual points represent separate neurons, and data comes from two (B) or three (D-E) separate culture preparations for each graph. One-way ANOVA with Tukey's multiple comparisons is used. All data shown as mean \pm SEM; ** $P < 0.01$, *** $P < 0.001$. (F) Representative images of hippocampal neurons showing ROIs with Ca^{2+} response (yellow)

rectangle, 10 μm) or without Ca^{2+} response (blue rectangle, 10 μm) when 100 ng/mL BDNF is perfused without and with 1 μM MPEP. (**G**) Left, representative image of hippocampal neuron expressing GCaMP8m (left, scale bar 10 μm), with snapshots of dendrites (white rectangle) during 500 nM VU-29 and 50 ng/mL BDNF perfusion (middle, scale bar 5 μm). Right, representative trace from 10 μm ROIs with Ca^{2+} response (yellow rectangle) from each dendrite.

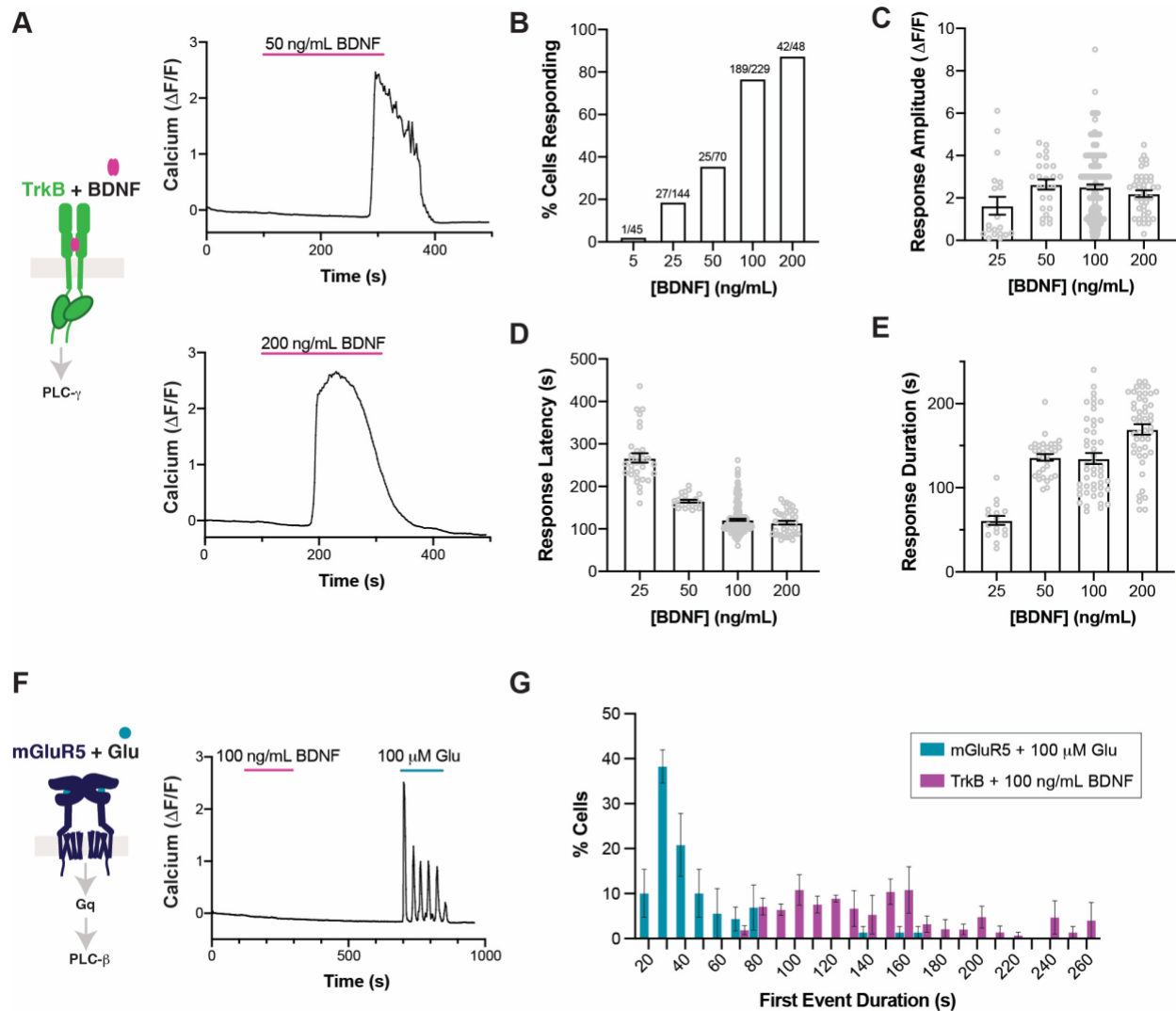


Figure S3. Characterization of BDNF-induced TrkB calcium signaling in HEK 293 cells, related to Figure 3. (A) Representative single-cell traces showing BDNF-induced Ca^{2+} responses in HEK 293-TrkB cells. (B-E) Bar graphs showing dose dependence of percentage of cells responding to BDNF (B), and the amplitude (C), latency (D), and duration (E) of responses. (F) Representative single-cell trace from a HEK 293 cell expressing mGluR5 only, showing no BDNF-induced Ca^{2+} response but a clear glutamate-induced oscillatory response. (G) Frequency distribution histogram of the percentage of cells with duration of the first Ca^{2+} event induced either by BDNF on HEK 293-TrkB cells or glutamate on HEK 293 cells transfected with mGluR5 only. The two distributions are significantly disparate by F test (34.95, Dfn 3, Dfd 20; $p < 0.0001$). For (C-E): individual points are individual cells, and data on each graph are from 3 separate cell preparations. One-way ANOVA with Tukey's multiple comparisons is used. All data shown as mean \pm SEM.

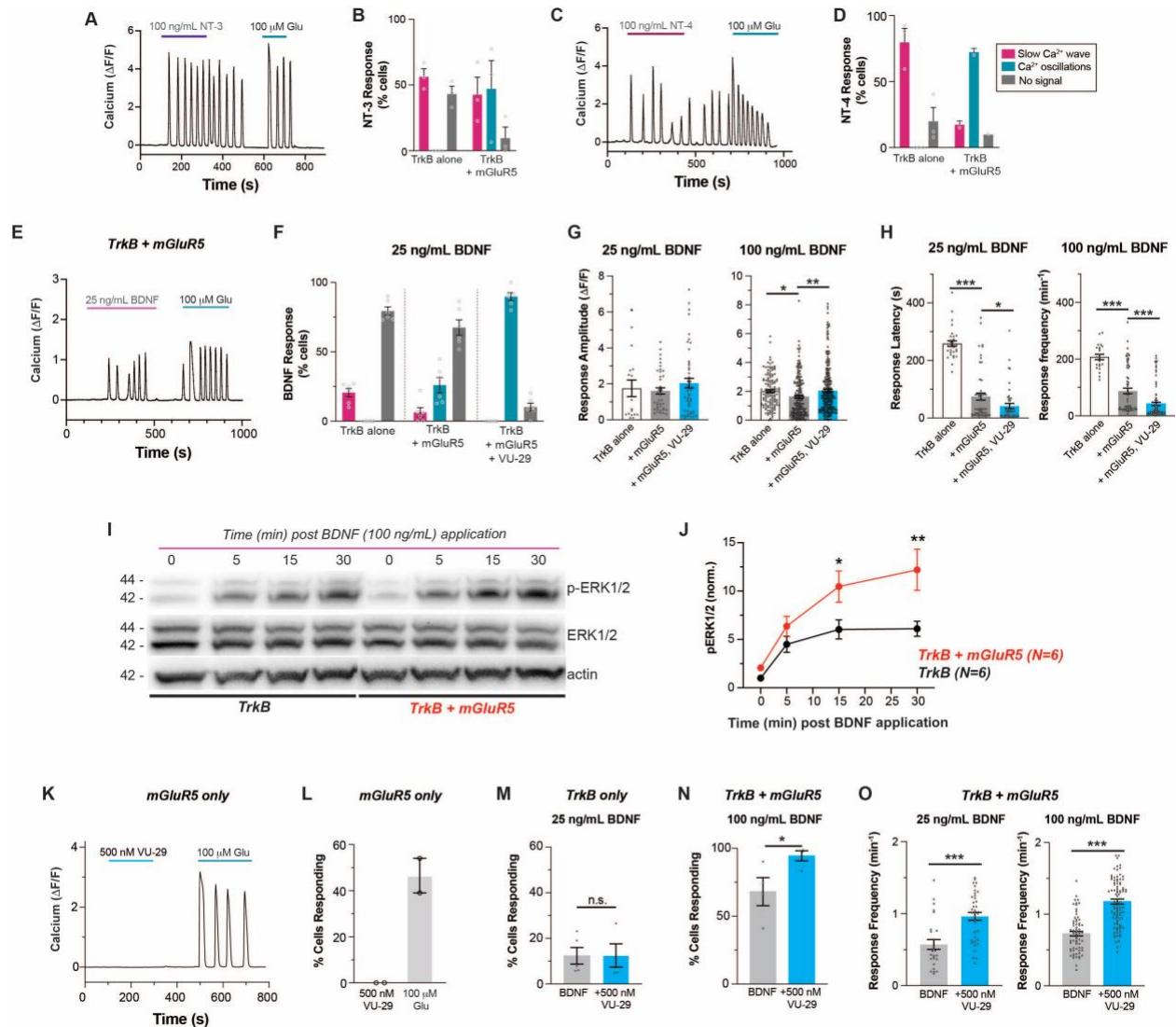


Figure S4. Further characterization of mGluR5 modulation of BDNF-induced TrkB signaling, related to Figure 3. (A-D) Representative traces and summary bar graphs showing NT-3-induced oscillatory Ca^{2+} responses (A-B) and NT-4 induced oscillatory Ca^{2+} responses (C-D) in HEK 293-TrkB cells expressing mGluR5. (E) Representative trace showing Ca^{2+} oscillations induced by low dose BDNF in HEK 293-TrkB cells transfected with mGluR5. (F) Distribution of BDNF-induced Ca^{2+} response with low dose of BDNF in HEK 293-TrkB cells with and without mGluR5 co-expression, as well as with and without co-application of 500 nM VU-29. (G-H) Bar graphs showing the effects of mGluR5 and 500 nM VU-29 on low dose (25 ng/mL) and high dose (100 ng/mL) BDNF response amplitude (G) and latency (H). (I-J) Representative western blot (I) and BDNF application time course graph (J) showing phospho-ERK1/2 response to BDNF in HEK 293-TrkB cells without and with mGluR5 co-expression. (n = 6 individual blots). (K-L) Representative trace (K) and summary bar graph (L) showing that 500 nM VU-29 alone does not elicit Ca^{2+} responses in HEK 293 cells expressing mGluR5 only. (M) Bar graph showing lack of any effect of co-application of VU-29 on percentage of cells responding to low dose BDNF (25 ng/mL) in HEK 293-TrkB cells without mGluR5 co-expression. (N) Bar graph showing effects of co-application of VU-29 with BDNF in HEK 293-TrkB cells with mGluR5 co-expression. Only cells

responding to glutamate were included in the graph. (O) Bar graphs showing that VU-29 increases the frequency of low dose and high dose BDNF-induced Ca^{2+} oscillations in HEK293-TrkB cells with co-expression of mGluR5. For (B), (D), (F), (L), (M), and (N): individual points come from separate coverslips. For (G), (H), and (O): individual points come from separate cells. For all conditions, data comes from at least 3 separate cell preparations. Two-way ANOVA with Sidak's multiple comparison test is used for (J). One-way ANOVA with Tukey's multiple comparison is used for (G) and (H). Unpaired t-test is used for (M), (N) and (O). All data shown as mean \pm SEM; * $P < 0.05$, ** $P < 0.01$, *** $P < 0.001$.

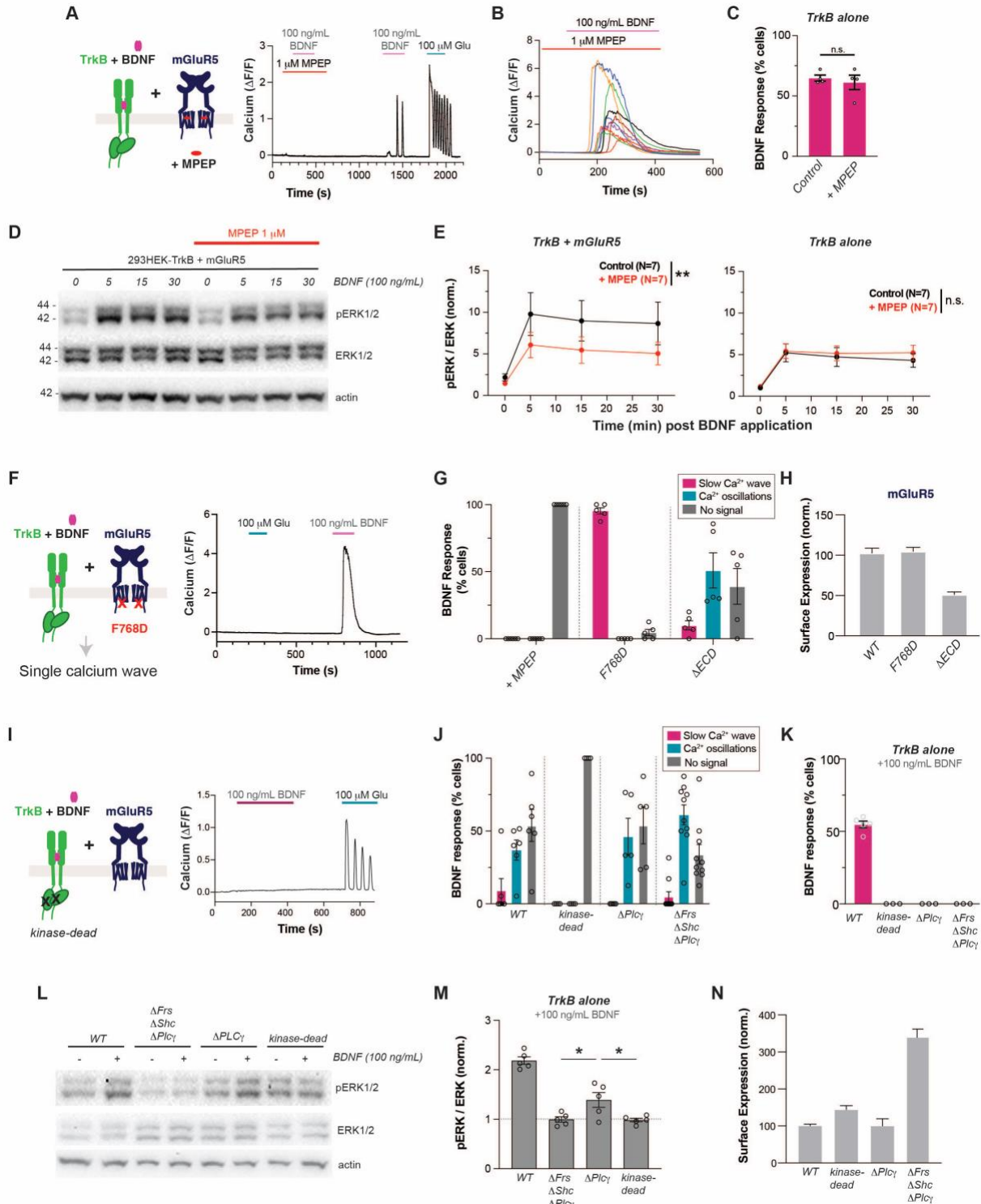


Figure S5. Sensitivity of BDNF-induced calcium oscillations to mGluR5 and TrkB perturbations, related to Figure 4. (A) Representative Ca^{2+} trace showing MPEP blocking BDNF-induced Ca^{2+} oscillations, followed by induction of BDNF-induced and glutamate-induced Ca^{2+} oscillations after MPEP washout. **(B-C)** Representative Ca^{2+} traces (B) and summary bar graph of percentage of cells responding to BDNF (C) showing that MPEP does not alter BDNF-induced Ca^{2+} signaling in HEK293-TrkB cells without mGluR5 co-expression. **(D-E)**

Representative western blot (D) and quantification (E) of BDNF-induced ERK activation in HEK 293-TrkB cells co-expressing mGluR5, showing a reduced response in the presence of MPEP. (F) Representative Ca^{2+} signaling trace with lack of BDNF and glutamate-induced Ca^{2+} oscillations in HEK 293 cells expressing mGluR5 F768D, a mutant mGluR5 with reduced affinity for G protein coupling. (G) Distribution of BDNF-induced Ca^{2+} responses in HEK 293-TrkB cells expressing mGluR5 WT with 1 μM MPEP, mGluR5 F768D, and mGluR5 ΔECD . (H) Bar graph showing normalized surface expression for mGluR5 WT, mGluR5 F768D, and mGluR5 ΔECD . (I) Representative trace showing the lack of BDNF-induced Ca^{2+} response in HEK 293 cells expressing TrkB kinase-dead and mGluR5, with maintained mGluR5 response to glutamate. (J) Distribution of Ca^{2+} response types in HEK 293 cells co-expressing mGluR5 with wild type or mutant TrkB. (K) Bar graph showing percentage of cells responding to BDNF in HEK 293 cells transfected with wild type or mutant TrkB. (L-M) Representative western blot (L) and quantification (M) of BDNF-induced ERK activation in HEK 293 cells transfected with TrkB wild type and mutants. BDNF (100 ng/mL) stimulation was done for 15 min. Quantification of pERK/ERK ratio shows BDNF-induced ERK activation as compared to each TrkB mutant baseline condition. (N) Bar graph showing the surface expression of TrkB mutants normalized to surface expression of wild type TrkB. For (C), (G), (J) and (K): individual points come from separate coverslips. For (M): individual points represent separate western blots with lysates prepared from disparate cell preparations. For all conditions, data comes from at least 3 separate cell preparations. Unpaired t-test is used for (C). Two-way ANOVA is used for (E). One-way ANOVA with Sidak's multiple comparisons is used for (M). All data shown as mean \pm SEM; * $P < 0.05$, ** $P < 0.01$.

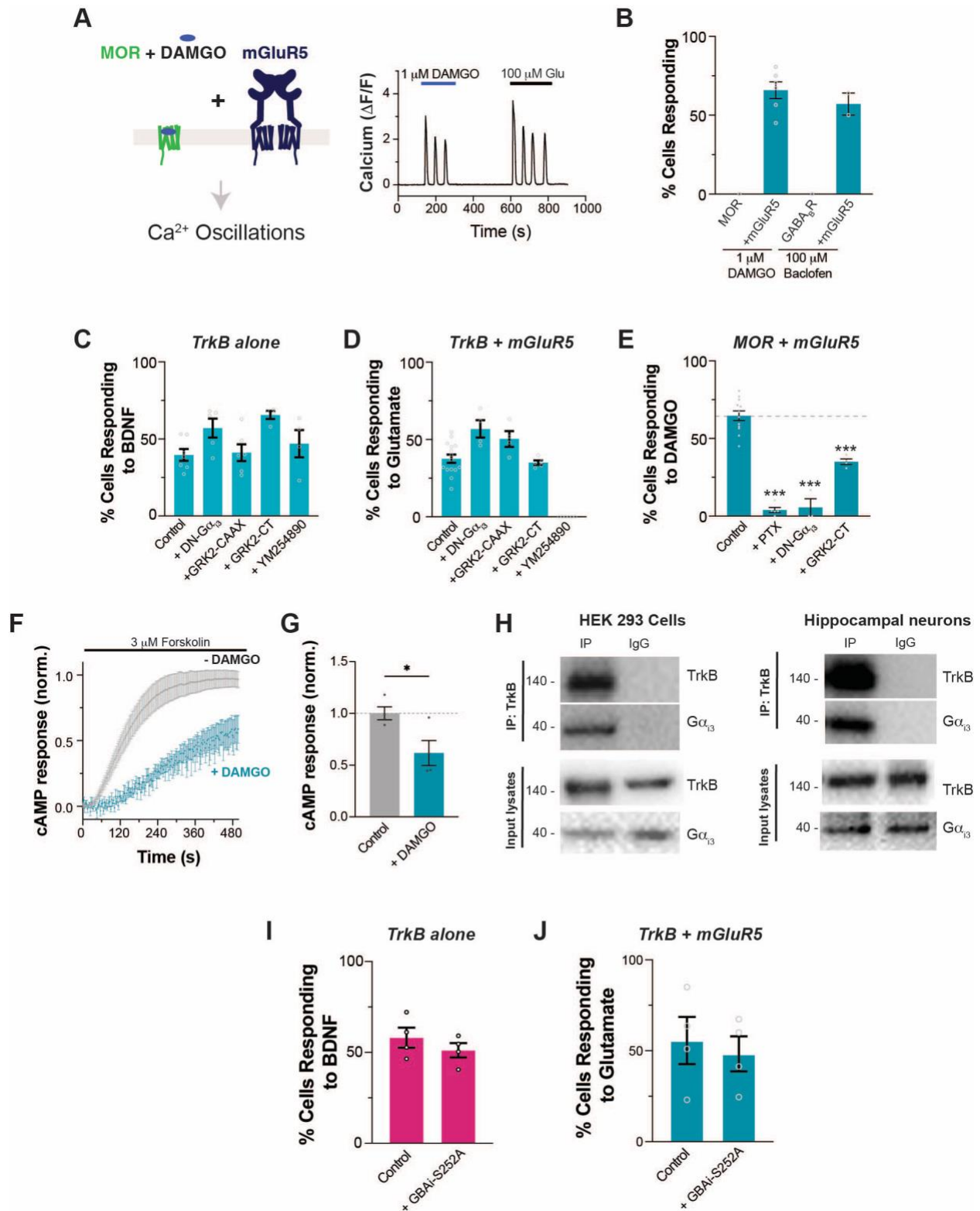


Figure S6. Further analysis of G protein synergy crosstalk model, related to Figure 5. (A) Representative trace showing DAMGO-induced Ca²⁺ oscillations in HEK 293 cells co-expressing MOR and mGluR5. **(B)** Summary bar graph of percentage of cells with agonist-induced Ca²⁺

response in HEK 293 cells expressing MOR or GABA_BR without or with mGluR5. **(C)** Summary bar graph showing the lack of effects of G protein perturbations and 20 μ M YM254890 on Ca²⁺ response to 100 ng/mL BDNF in HEK 293-TrkB cells without mGluR5 co-expression. **(D)** Summary bar graph showing the percentage of HEK 293-TrkB cells with mGluR5 co-expression showing 100 μ M glutamate-induced Ca²⁺ responses. G protein perturbations show no clear effect on glutamate response, except for YM254890 (20 μ M). **(E)** Summary bar graph showing decreased responses to 1 μ M DAMGO in HEK 293 cells co-expressing MOR and PTX, DN-G α_{i3} , or GRK2-CT with mGluR5. **(F-G)** Normalized traces (F) and summary bar graph (G) showing forskolin-induced cAMP response in HEK 293 cells expressing MOR with or without co-application of 1 μ M DAMGO. **(H)** Representative co-immunoprecipitation blots of TrkB and G α_{i3} protein in HEK293-TrkB cells and primary hippocampal neurons. Both samples were treated with BDNF 100 ng/mL for 15 min. **(I-J)** Summary bar graph showing the effects of co-expression of GBAl-S252A on percentage of cells responding to BDNF in HEK293-TrkB cells without mGluR5 co-expression (I) or glutamate in HEK293-TrkB cells with mGluR5 co-expression (J). For (B), (C), (D) (E), (G), (I) and (J): Individual points come from separate coverslips from at least 3 separate cell preparations. One-way ANOVA with Dunnett's multiple comparison test is used to compare with control group for (C), (D), and (E). Unpaired t-test was used for (G), (I), and (J). All data shown as mean \pm SEM; * P < 0.05, *** P < 0.001.

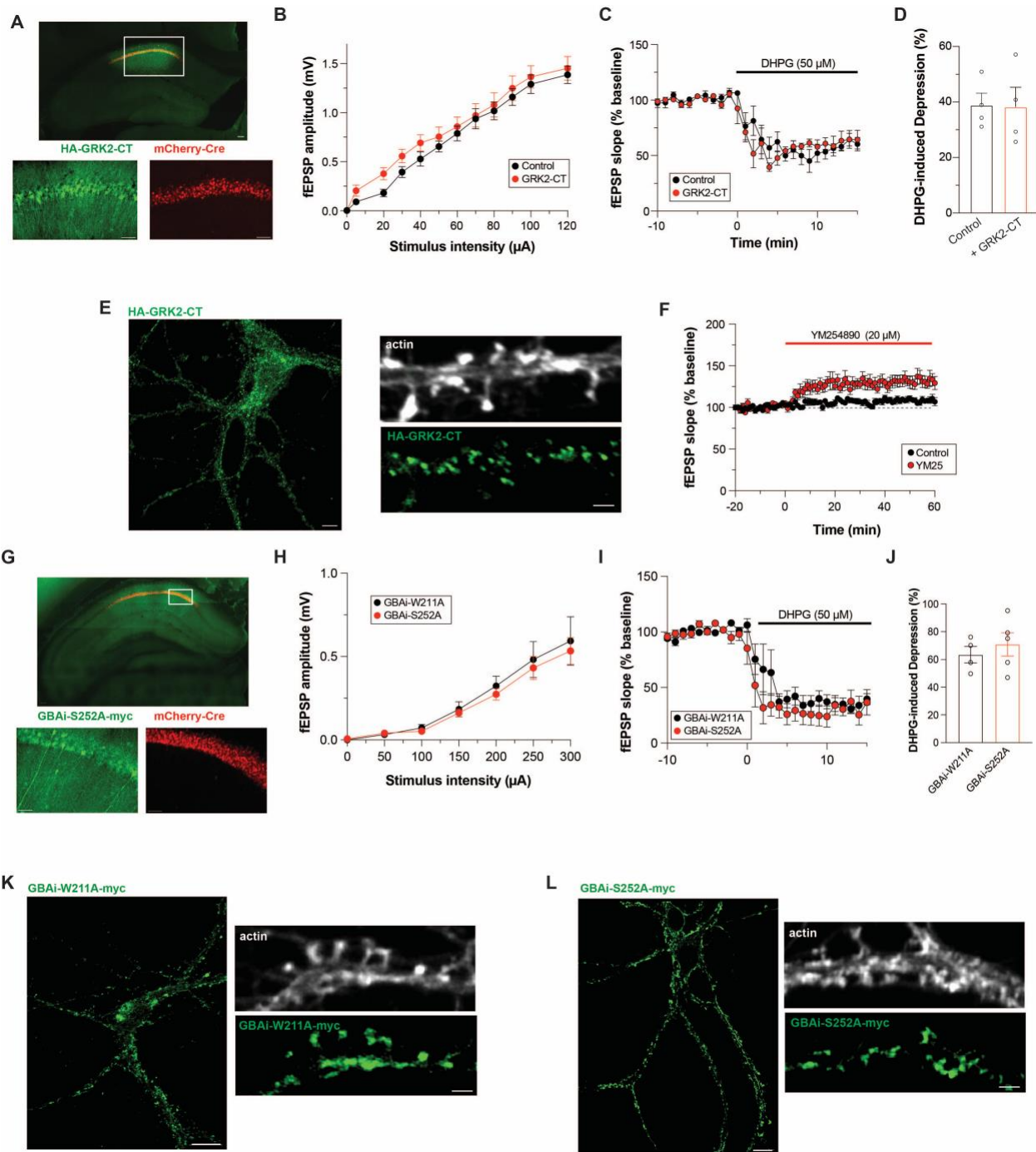


Figure S7. Further analysis of G protein-perturbations on BDNF-driven synaptic plasticity, related to Figure 6. (A) Representative confocal image of the hippocampus, showing expression of CaMKII-mCherry-Cre and HA-GRK2-CT in the dorsal CA1 (top, scale bar 100 μ m). Close-up of the dorsal CA1 region (top, white rectangle) shown with soma and dendritic filling of the HA-GRK2-CT and mCherry-Cre (bottom, scale bar 50 μ m). (B) Input/output curve of fEPSP amplitude showing no change in basal synaptic strength upon expression of HA-GRK2-CT (n = 4 slices). (C-D) fEPSP slope time course (C) and summary bar graph (D) showing no effects of HA-GRK2-

CT expression on DHPG induced synaptic inhibition. Individual points represent independent slices taken from distinct mice. **(E)** Representative confocal image of HA-GRK2-CT expression in primary hippocampal neurons (left, scale bar 5 μm) with a zoom-in of the dendritic shaft (right, scale bar 1 μm). **(F)** Incubation with YM-254890 elicits a modest increase in fEPSP slope that stabilizes within 20 min ($n = 6$ slices from distinct mice). **(G)** Representative confocal image of the hippocampus, showing expression of GBai-S252A-myc and CaMKII-mCherry-Cre in the dorsal CA1 (top, scale bar 100 μm). Close-up of the dorsal CA1 region (top, white rectangle) shown with soma and dendritic filling of the GBai-S252A-myc (bottom, scale bar 50 μm). **(H)** Input/output curve of fEPSP amplitude in slices injected with GBai-W211A ($n = 6$ slices) and GBai-S252A ($n = 5$ slices). **(I-J)** fEPSP slope time course (I) showing that DHPG application decreases fEPSP slope in slices expressing GBai-W211A ($n = 4$ slices) and GBai-S252A ($n = 5$ slices). In (I), grey bars show regions averaged for baseline and post-BDNF values in (J). For (D) and (J), unpaired t-test is used. All data shown as mean \pm SEM.

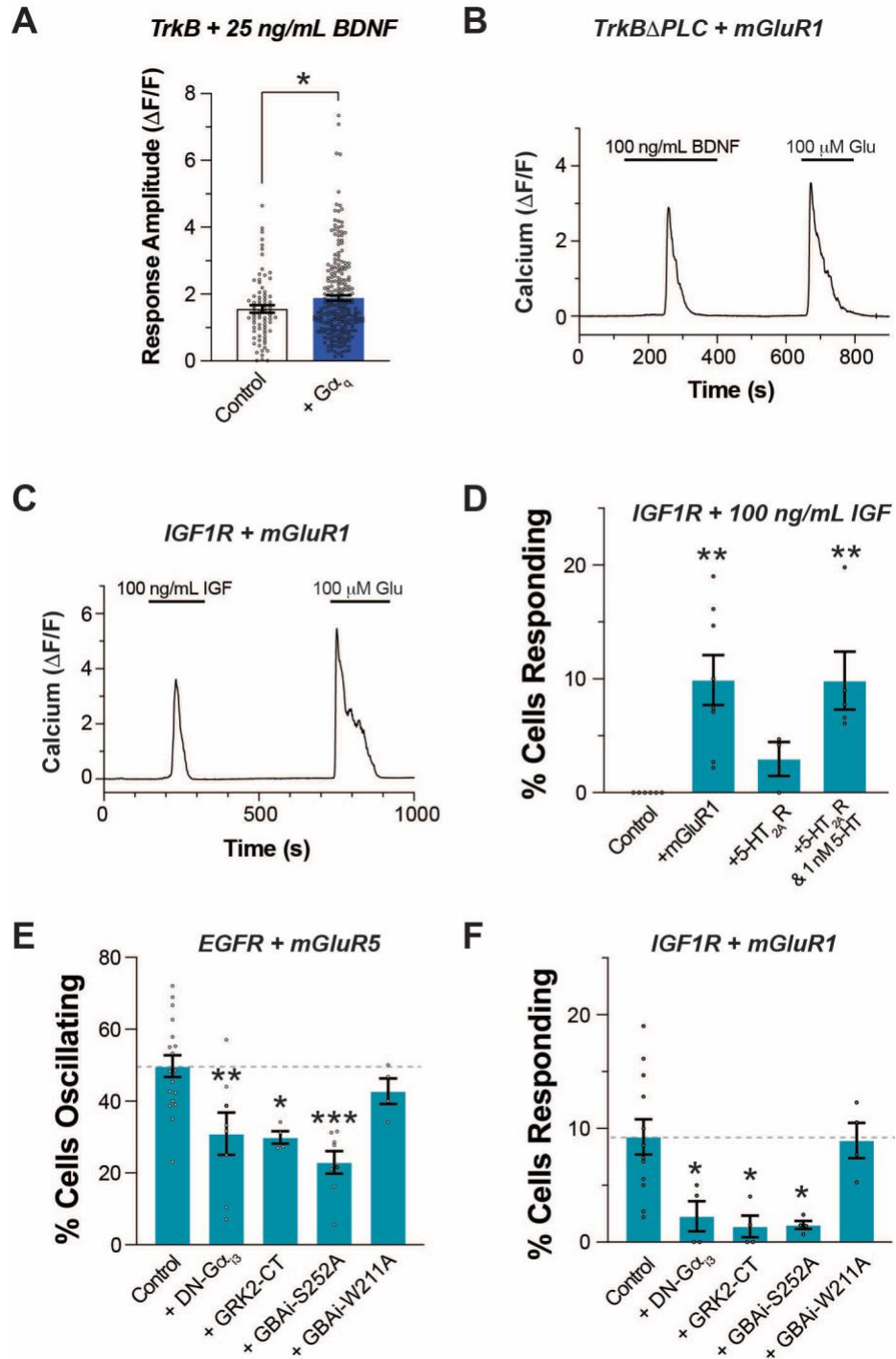


Figure S8. Further analysis of G protein-perturbations on RTK/GPCR crosstalk, related to Figure 7. (A) Bar graph showing the effects of $G\alpha_q$ co-expression on low dose BDNF-induced calcium response amplitude in HEK293-TrkB cells. (B) Representative trace showing BDNF-induced Ca^{2+} response in HEK 293 cells co-expressing TrkB- Δ PLC γ (B) or IGF $_1$ R (C) and mGluR1. (D) Summary bar graph showing percentage of cells responding to IGF in HEK 293 cells co-expression of IGF $_1$ R and mGluR1 or 5-HT $_2A$ R. (E) Summary bar graph showing decreased responses to 100 ng/mL EGF in HEK 293 cells co-expressing mGluR5 and DN- $G\alpha_{13}$, GRK2-CT or

GBAi-S252A but not GBAi-W211A. (F) Summary bar graph showing decreased responses to 100 ng/mL IGF in HEK 293 cells co-expressing IGF₁R, mGluR1 and DN-Gα_{i3}, GRK2-CT, or GBAi-S252A but not GBAi-W211A. Only cells responding to glutamate or 5-HT were included for (D), (E) and (F). Unpaired t-test is used for (A). One-way ANOVA with Dunnett's multiple comparison test is used to compare with control group for (D), (E) and (F). All data shown as mean ± SEM; * P < 0.05, *** P < 0.001.